

PROCEEDINGS OF SPIE

[SPIDigitalLibrary.org/conference-proceedings-of-spie](https://spiedigitallibrary.org/conference-proceedings-of-spie)

Precision astrometry with adaptive optics

P. B. Cameron, M. C. Britton, S. R. Kulkarni

P. B. Cameron, M. C. Britton, S. R. Kulkarni, "Precision astrometry with adaptive optics," Proc. SPIE 7015, Adaptive Optics Systems, 70150A (7 July 2008); doi: 10.1117/12.789811

SPIE.

Event: SPIE Astronomical Telescopes + Instrumentation, 2008, Marseille, France

Precision astrometry with adaptive optics

P. B. Cameron, M. C. Britton and S. R. Kulkarni

California Institute of Technology, Pasadena, CA 91125

ABSTRACT

We discuss the limits of ground-based astrometry with adaptive optics based on experiments using the core of the Galactic globular cluster M5. We have recently achieved $\lesssim 100$ microarcsecond astrometric precision and accuracy at the Hale 200-inch telescope. Here we apply the same experimental design considerations and optimal estimation technique to explore the astrometric precision of the Keck II telescope. We find that high-precision astrometry at ≈ 50 microarcsecond level is possible at Keck in 20 seconds. We discuss the potential of differential astrometry for current and next generation large aperture telescopes based on these results.

Keywords: adaptive optics; astrometry; globular clusters: individual (M5)

1. INTRODUCTION

Ground-based adaptive optics (AO) offer an easily accessible and cost effective method for overcoming atmospheric turbulence over small fields (\lesssim arcminute). Current astronomical adaptive optics systems provide diffraction-limited image quality at near-infrared wavelengths. Achieving the telescope's diffraction limit and the resulting boost in signal-to-noise ratio prove to be a powerful combination for astrometry. These two effects reduce the errors in determining stellar centers, increase the number of possible reference stars at small separations, and allow techniques for mitigating systematics.

We have used these facts with great success recently at the Hale 200-inch telescope to achieve astrometry at levels previously reserved for interferometers.¹ The increase in sky coverage from laser technology and improved wavefront sensors, operation in the near-infrared, gain in signal-to-noise ratio (SNR), and the diffraction-limited image quality make astrometry with adaptive optics amenable to numerous Galactic applications spanning a wide range of fields: detection of astrometric companions, the improved determination of the mass-luminosity relation of stars, and the formation and evolution of compact objects.²

Here we apply the optimal estimation technique appropriate for mitigating the astrometric errors arising in AO observations to images of the core of the globular cluster M5 using the Keck II telescope. We achieve $\sim 50 \mu\text{as}$ astrometric precision in 20 seconds. In §2 we review the dominant systematic errors that arise in ground-based astrometry and the experimental techniques we have adopted to control them. We summarize the framework of our reduction model in §3. We describe the observations of M5 and the results of applying the optimal estimation technique to the data in §4 and §5. This is followed in §6 by a discussion of the role and potential of adaptive optics in ground-based astrometry with current and future large aperture telescopes.

2. SYSTEMATIC EFFECTS

Ground-based astrometric measurements are typically limited by effects that systematically alter the differential offsets between stars. Both the atmosphere and instrumentation have contributions that must be considered. Observations with adaptive optics benefit from a substantial SNR gain, and thus data can be taken efficiently to help mitigate these effects. Below we enumerate the largest contributors to systematic errors.

Further author information: send correspondence to pbc@astro.caltech.edu

2.1 Distortion

The largest instrumental systematic error in any optical system is geometric distortion. Even the most careful design considerations cannot achieve accurate image placement at the levels measurable with AO astrometry. It is necessary to map the static geometric distortions, and often even track any dynamic distortions (e.g. due to flexure of an instrument mounted at the Cassegrain focus).

If geometric distortions are stable, two strategies can be used to eliminate their effect on data sets acquired with a single instrument. The first is to model the distortion to high accuracy and apply a correction (e.g. Ref. 3). This is clearly essential for data obtained using multiple instruments to place them in a global astrometric frame. The second technique is to use the same optical prescription at each epoch. Namely, place the field at the same location and orientation on the detector and dither only minimally, if at all. Here we use both a distortion solution and a single, consistent dither position to achieve precise, accurate astrometry.

Both the Palomar and Keck near-infrared images have their distortions mapped to high accuracy*. The Palomar distortion solution includes a term to compensate for flexure in the AO bench and imager due to its location at the Cassegrain Focus. The Keck imager, located on the Nasmyth deck, includes no such correction. The long-term stability of these systems are best addressed with on-sky data, which was one of the purposes of the observations discussed here.

2.2 Atmospheric Refraction

Refraction by the Earth's atmosphere causes an angular deflection of light from a star, resulting in an apparent change in its position. The magnitude of this deflection depends on the wavelength and the atmospheric column depth encountered by an incoming ray. The former effect is chromatic, while the latter is achromatic. The error induced by differential chromatic refraction (DCR) has proven to be an important, and sometimes the dominant, astrometric limitation in ground-based efforts (e.g. Refs. 4–7). These studies have shown DCR can contribute ≈ 0.1 – 1 mas of error depending on the wavelength and strategy of the observations.

The observations for Palomar were conducted using a Br- γ filter at $2.166\,\mu\text{m}$ with a narrow bandpass of $0.02\,\mu\text{m}$ to suppress differential chromatic refraction. The increased signal-to-noise ratio provided by adaptive optics allows sufficient reference stars to be detected even through such a narrow filter in a short exposure time. We reach $K_s \approx 15$ magnitude in our 1.4 s exposures through this filter with the Hale 200-inch (see §4). In addition, observations were acquired over a relatively narrow range of airmass (1.17–1.27) at each epoch to minimize the achromatic differential refraction.

Keck observations were performed over a small range of zenith angles (airmass = 1.11–1.09), but a broadband filter was used (K'). For both Palomar and Keck we used the *slarefro* function in the STARLINK library to estimate the magnitude of refraction effects.⁸ In each case, the effect should be negligible ($\lesssim 10\,\mu\text{as}$).

3. MEASUREMENT MODEL

The goal of an astrometric measurement model is to determine the position of a target relative to a grid of N reference stars, and ideally reach the ultimate limit set by one's ability to measure the center of the astrometric target. A perfect detector and optics free from the systematic effects mentioned in §2 would deliver a centering precision of

$$\sigma_{\text{meas}} = \frac{\lambda}{\pi D} \frac{1}{\text{SNR}} = 284\,\mu\text{as} \left(\frac{\lambda}{2.17\,\mu\text{m}} \right) \left(\frac{5\,\text{m}}{D} \right) \left(\frac{100}{\text{SNR}} \right) \quad (1)$$

(Ref. 9). For AO observations, Equation 1 is overly optimistic due to uncertainties in the estimation of the AO point-spread function (PSF). A number of software and analytic efforts have been aimed at reducing natural guide star AO data (e.g. Ref. 10, 11). Here we have not adopted these programs, instead relying on widely-used astronomical software (IRAF), and concentrating on the largest astrometric error source, differential atmospheric tilt jitter (see below). The adoption of better centering algorithms could improve the results presented here.

*see <http://www.astro.ucla.edu/~metchev/ao.html> and http://www2.keck.hawaii.edu/inst/nirc2/forReDoc/post_observing/dewarp/

Nonetheless, we are able to determine stellar centers at the 0.01–0.05 pixel level, and these errors decrease as the square root of the number of images.

The ideal limit set by Equation 1 is degraded by the presence of uncorrected atmospheric turbulence, and uncertainties in positional determination due to the density and geometry of the grid of reference stars. Here we will summarize an optimal estimation technique aimed at mitigating these two effects.

The fundamental quantities in differential astrometry are the measured angular offsets between the astrometric target (i) and the reference stars (j), written

$$\vec{d}_{ij} = \begin{bmatrix} x_j - x_i \\ y_j - y_i \end{bmatrix} \equiv \begin{bmatrix} x_{ij} \\ y_{ij} \end{bmatrix}, \quad i \neq j, \quad (2)$$

where $x_{ij} \equiv x_j - x_i$, and likewise for y . We can combine these measurements into a single column vector. For target star ‘0’ this would be

$$\mathbf{d} = [x_{01}, \dots, x_{0N}, y_{01}, \dots, y_{0N}]^T. \quad (3)$$

The position (\mathbf{p}) of the astrometric target relative to the grid of reference stars can be described by a linear combination of weightings \mathbf{W} , such that

$$\mathbf{p} = \mathbf{W}\mathbf{d}. \quad (4)$$

Here

$$\mathbf{W} = \begin{bmatrix} w_{xx,01} & \cdots & w_{xx,0N} & w_{xy,01} & \cdots & w_{xy,0N} \\ w_{yx,01} & \cdots & w_{yx,0N} & w_{yy,01} & \cdots & w_{yy,0N} \end{bmatrix}. \quad (5)$$

We have used the notation $w_{xy,0i}$ to denote the weighting of the offset from the target star to star i in the y direction used to determine the x component of the target’s position, \mathbf{p} . For example, for a standard average of the x and y measurements to calculate \mathbf{p} , we would assign all the $w_{xx,0i} = w_{yy,0i} = 1/N$ and $w_{xy,0i} = w_{yx,0i} = 0$.

The quantity \mathbf{p} represents the position of the astrometric target in the sense that any proper motion of the target, ϵ , with respect to the fixed grid between two epochs will cause a change, $\mathbf{p} \rightarrow \mathbf{p} + \epsilon$, if the weights are subject to the constraints that

$$\sum_i w_{xx,0i} = 1, \quad \sum_i w_{yy,0i} = 1, \quad \sum_i w_{xy,0i} = 0, \quad \sum_i w_{yx,0i} = 0. \quad (6)$$

Note that there is nothing constraining these weights to be positive. Allowing the subtraction and scaling of certain measurements effectively allows the distribution of reference stars to be symmetrized in order to eliminate noise.

In this formalism, each instance of \mathbf{d} (each image) is drawn from a multivariate normal distribution with covariance matrix $\Sigma_{\mathbf{d}}$. The statistics of the positional measurements \mathbf{p} are described by the eigenvalues and eigenvectors of the matrix

$$\Sigma_{\mathbf{p}} = \mathbf{W}^T \Sigma_{\mathbf{d}} \mathbf{W}. \quad (7)$$

Thus, it is necessary to have knowledge of the covariance matrix, $\Sigma_{\mathbf{d}}$, by either calculating it theoretically, or by estimating it directly from data. One then wishes to use this knowledge to choose the weights, \mathbf{W} , that minimize the trace of $\Sigma_{\mathbf{p}}$ using, for example, the method of Lagrange multipliers.^{1,12}

For the observations presented here, and as is often the case in AO astrometric observations, the dominant random error is a consequence of tilt anisoplanatism. More specifically, in propagating through the atmosphere to reach the telescope aperture, light from the target star and light from a reference star at a finite angular offset traverse different columns of atmospheric turbulence that are sheared. Differential atmospheric tilt jitter arises from the decorrelation in the tilt component of the wavefront phase aberration arising from this shearing effect. This differential tilt leads to a random, achromatic, and anisotropic fluctuation in the relative displacement of the two objects. The three term approximation to the parallel and perpendicular components of the variance arising from differential atmospheric tilt jitter, assuming Kolmogorov turbulence, is given by¹³

$$\begin{bmatrix} \sigma_{\parallel, \text{TJ}}^2 \\ \sigma_{\perp, \text{TJ}}^2 \end{bmatrix} = 2.67 \frac{\mu_2}{D^{1/3}} \left(\frac{\theta}{D} \right)^2 \begin{bmatrix} 3 \\ 1 \end{bmatrix} - 3.68 \frac{\mu_4}{D^{1/3}} \left(\frac{\theta}{D} \right)^4 \begin{bmatrix} 5 \\ 1 \end{bmatrix} + 2.35 \frac{\mu_{14/3}}{D^{1/3}} \left(\frac{\theta}{D} \right)^{14/3} \begin{bmatrix} 17/3 \\ 1 \end{bmatrix}. \quad (8)$$

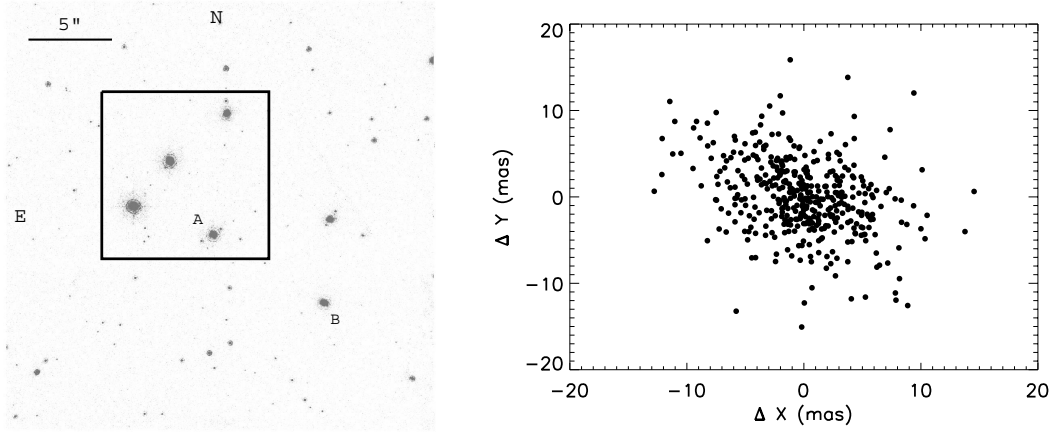


Figure 1. *Left Panel:* Image of the core of the globular cluster M5 in 1.4 seconds through the narrow-band Br- γ filter at the Hale 200-inch telescope with orientation North up and East to the left. The AO guide star is labeled as star 'A', and is one of 82 detected stars in the image. The dark box denotes the field of observed by the NIRC2 narrow-channel which contains 20 stars. *Right Panel:* Deviation from the mean separation in each of the ≈ 400 images of stars 'A' and 'B' as observed from Palomar on 2007 May 29. The measured separations show the clear signature of anisotropic differential atmospheric tilt jitter as predicted from Equation 8. However, the magnitude is less than expected from DIMM/MASS estimates of the turbulence profile, indicating some temporal averaging during a 1.4 sec exposure.

In this equation D is the telescope diameter and θ is the angular separation of the stars. The turbulence moments μ_m are defined as

$$\mu_m = \sec^{m+1} \xi \int_0^\infty dh C_n^2(h) h^m, \quad (9)$$

where h is the altitude, ξ is the zenith angle, and $C_n^2(h)$ is the vertical strength of atmospheric turbulence. Typical $C_n^2(h)$ profiles yield $\sigma_{\parallel, \text{TJ}} \approx 10\text{--}20\text{ mas}$ for a $20''$ binary when observed with a 10 m aperture. Note that the variance from differential tilt is a random error, and thus is also $\propto \tau_{\text{TJ}}/t$, where τ_{TJ} is the tilt jitter timescale (of order the wind crossing time over the aperture) and t is the integration time. The theoretical covariance matrix due to differential atmospheric tilt jitter can be found in Ref. 1.

4. OBSERVATIONS

We observed the central region of the Galactic globular cluster M5 using the Hale 200-inch telescope and the Palomar High Angular Resolution Observer (PHARO; Ref. 14) assisted by the Palomar Adaptive Optics System (PALAO; Ref. 15), as well as the Keck II Telescope equipped with adaptive optics and the Near Infrared Camera 2.¹⁶ The Palomar observations are described in detail elsewhere,¹ here we focus on the observations 2007 May 29 in comparison with Keck observations from 2007 June 11. At Palomar, M5 was imaged through the narrow-band Br- γ filter (central wavelength is $2.166\text{ }\mu\text{m}$ and bandpass is $0.02\text{ }\mu\text{m}$) using the $25'' \times 25''$ narrow-field channel ($0.025''/\text{pixel}^{-1}$) with a 1.4 sec exposure time, and ≈ 400 total images. An image of the field can be found in Figure 1.

The Keck observations were obtained with correlated double sampling of the detector with an effective integration time of 1 sec per image (0.2 sec exposure time with 5 on-chip co-additions), a broadband K' filter, and the narrow-field channel ($\approx 10'' \times 10''$; $9.942\text{ mas pix}^{-1}$), which substantially over samples the diffraction limited PSF ($\approx 50\text{ mas}$ full width at half maximum) of the Keck II telescope. These observations yielded 100 images. This substantial over sampling and the properties of the NIRC2 and PHARO detectors lead to essentially the same SNR of detection stars in both the Keck and Palomar images.

As with the Palomar data, we processed the raw Keck images by subtracting dark frames and removing bad pixels from the analysis. Flat-field calibration was performed using twilight sky flats. Sky subtraction was accomplished by forming the median of the dithered frames taken outside of the cluster and subtracting this

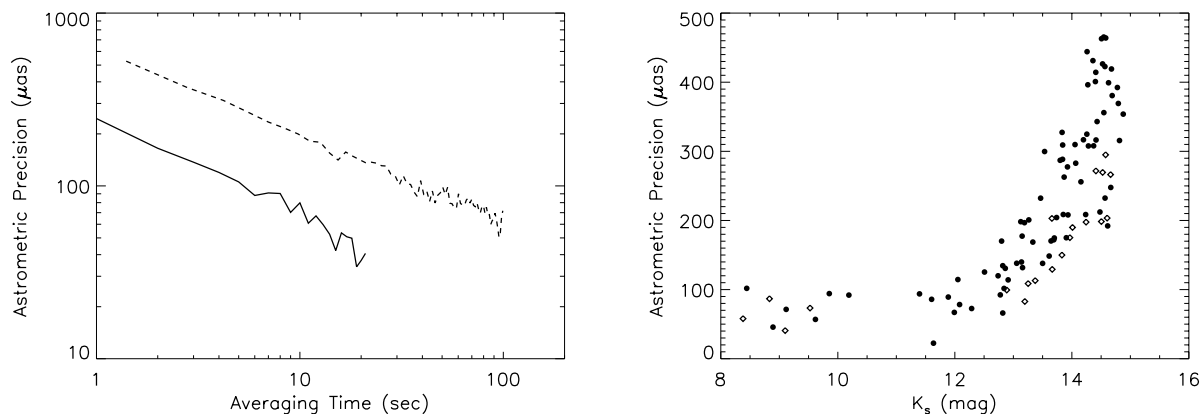


Figure 2. *Left Panel:* Geometric mean of the Allan deviation in each axis of the guide star position as a function of integration time for the Palomar observations of 2007 May 29 (dashed curve) and the Keck observations of 2007 June 11 (solid curve). The astrometric precision improves as $1/\sqrt{t}$, and the centering precision increases by the expected factor of ≈ 2 predicted with the doubling of aperture diameter between Keck and Palomar (Equation 1). *Right Panel:* The astrometric precision (Allan deviation after 2 minutes for Palomar; after 20 seconds for Keck) as function of K_s magnitude for all 82 detected stars on Palomar (filled circles) 2007 May 29 and 20 stars at Keck (open diamonds) on 2007 June 11. The precision in both cases is essentially constant for $K_s \lesssim 13$ mag.

median from each exposure. The photometry and astrometry of each star was extracted using PSF-fitting as implemented by the DAOPHOT package in PyRAF[†].

5. RESULTS

In Figure 1 we see the residuals of the measured offset between a pair of stars in the core of M5. The residuals show the characteristic signature of differential tilt jitter. Namely, the RMS separation along the axis connecting the two stars is larger than that of the perpendicular axis by a factor of $\approx \sqrt{3}$, and that this effect is the dominant astrometric error. It is slightly smaller than the expected theoretical magnitude, but this is likely due to some tilt averaging during the ~ 1 sec exposures.

5.1 Astrometric Precision

The astrometric precision achieved in a single epoch is an important diagnostic of the measurement model. On a given night for a given star, we use the 100–500 images to derive the covariance matrix for each target star, Σ_d , and use it to determine the optimal weights. We then apply this weight matrix to the measured offsets to compute the target’s position in each image — resulting in a timeseries in each component of \mathbf{p} for each epoch. The properties of each timeseries are best explored by computing its Allan deviation. The Allan deviation is calculated by dividing a timeseries into chunks, averaging each segment, and computing the RMS of the resulting, shorter timeseries. If the timeseries is dominated by random errors, its Allan deviation will decrease as $1/\sqrt{t_{\text{avg}}}$, where t_{avg} is the length of each chunk. It is also necessary to have sufficiently many segments so that an RMS calculation is meaningful. For Palomar, the longest timescale probed is ≈ 2 minutes for the total 10 minute timeseries. For Keck, we have only 100 sec, so the longest timescale probed is ≈ 20 sec.

We compute the geometric mean of the Allan deviation in each dimension as a function of the averaging time for the AO guide star in Figure 2 after computing the covariance matrix from data. After 1.4 seconds the guide star’s positional precision is $\approx 550 \mu\text{as}$. The precision subsequently improves as $t^{-1/2}$ to $\approx 70 \mu\text{as}$ after 2 minutes, and has yet to hit a systematic floor. This suggests a precision of $\approx 30 \mu\text{as}$ for the full 10 minute data set, assuming that no systematic limit is reached in the interim. At Keck, we reach the $250 \mu\text{as}$ in 1 sec, and

[†]PyRAF is a product of Space Telescope Science Institute, which is operated by AURA for NASA.

improve to the $50\text{--}60\,\mu\text{s}$ level in only 20 seconds. This suggests a precision of $\approx 25\,\mu\text{s}$ with the full 100 frames. The ratio of precisions agrees well with expectation of a factor of 2 improvement due to the aperture diameter size increase (given the comparable signal-to-noise ratios of the detections).

This level of precision is not limited to the AO guide star; similar performance is obtained on other stars in the core of M5. In Figure 2 we show the astrometric precision obtained on 2007 May 29 at Palomar after 2 minutes and on 2007 June 11 after 20 seconds for all detected stars as a function of their K_s magnitude. The precision below $100\,\mu\text{s}$ achieved on targets as faint as $K_s \approx 13$ magnitude using these short individual exposures demonstrates the substantial signal-to-noise ratio benefit afforded by adaptive optics.

Clearly, it is desirable to obtain a sufficient number of frames ($\gg N$) to calculate the covariance matrix, Σ_d , from data. However, we have previously demonstrated that high-precision astrometry is possible even when observers lack a sufficient number of images. An independent estimate of the turbulence profile (e.g. from a DIMM/MASS unit^{17,18}) during the observations can be used to calculate this matrix theoretically, and achieve astrometric performance within a factor of 2–4 of that presented here.¹

5.2 Astrometric Accuracy

The goal of astrometry is to measure the position of the target star over time spans ranging from hours to years. For these experiments to be viable it is necessary for the optical systems to be stable over these periods. There are several obstacles that could render the single-epoch precision obtained in §5.1 meaningless. For example, PHARO is mounted at the Cassegrain focus which results in flexure of the instrument as the telescope tracks, and undergoes warming and cooling cycles between observing periods (typically twice per month) that could cause small changes in the powered optics. Either of these facts could alter the geometric distortion, and make astrometric measurements unrepeatable. Our Palomar experiment was designed to be as consistent as possible and spanned many removal and reinstallations of PHARO over 2 months. The observations were shown to be repeatable at the $\approx 100\,\mu\text{s}$ level.¹ This somewhat worse than expected given the achieved precision, but would still allow a number of very interesting astrometric programs to be carried out.

The Keck AO system and NIRC2 has the potential for being much more stable. Both are mounted in static positions on the Nasmyth deck, and NIRC2 is maintained at a constant temperature. Unfortunately, we do not have adequate data to evaluate the astrometric stability of the Keck system over long time baselines to the level of precision presented here. We do monitor the system stability with observations of M5, but our scientific program is aimed at achieving astrometry of compact objects at the $\approx 1\text{ mas}$ level.¹⁹ As such, our other M5 observations contain only a few images for comparison purposes. However, can confirm the system is accurate enough to perform milliarcsecond level astrometry on timescales of years.

6. DISCUSSION AND CONCLUSIONS

Here have illustrated the high levels of astrometric performance that are possible using ground-based telescopes equipped with adaptive optics systems. With AO, the effects of distortion and atmospheric dispersion that give rise to systematic errors can be mitigated through experimental design. Random errors arising from differential tilt jitter and measurement noise can be minimized through the use of an optimal estimation scheme that accounts for the correlated noise statistics through the covariance matrix, Σ_d . However, the measurement model is general, in that it can accommodate any random noise source that effects differential measurements, and determines how these measurements can be optimally combined. The experimental results obtained on the Hale 200-inch and Keck II Telescopes have demonstrated single epoch astrometric precision of $\lesssim 100\,\mu\text{s}$ and accurate multi-epoch performance.¹ This level of precision is comparable to that afforded by ground-based interferometry.

Simulations of astrometric precision afforded by the optimal weighting scheme have shown that measurement noise is the dominant residual astrometric error on a 5 meter telescope for stellar fields that contain more than a few reference stars. The scaling laws for differential tilt jitter ($D^{-7/6}$) and measurement noise (D^{-2}) indicate that on larger aperture telescopes measurement noise will represent a smaller fraction of this residual error. This effect is illustrated in Figure 3, which shows the RMS error between pairs of stars for a range of telescope apertures and angular separations.

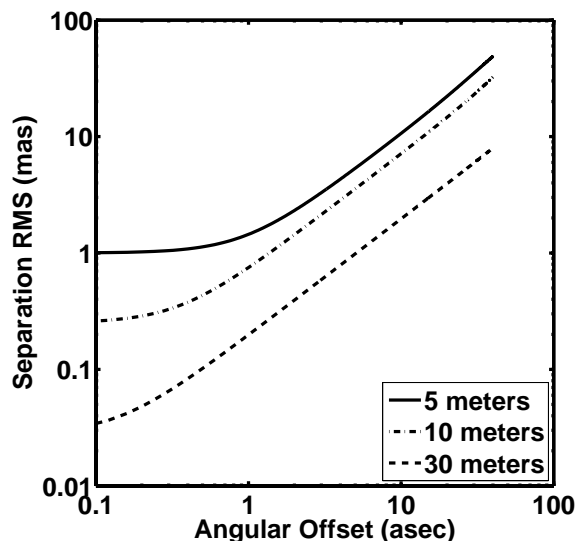


Figure 3. The RMS separation between a pair of stars versus angular offset and aperture diameter. We have assumed a typical Palomar turbulence profile, a centering error of $1/\sqrt{2}$ mas for each star for a 5 m telescope, and included the geometric mean of each component of Equation 8. Relative to Palomar (solid curve), there are substantial astrometric gains to be made for larger 10 m (dash dotted) and 30 m (dashed) telescopes due to the reduction of both measurement noise (the y -intercept; $\propto D^{-2}$) and tilt jitter ($\propto D^{-7/6}$). Because measurement noise falls off more quickly with D , tilt jitter becomes the dominant source of astrometric error for large aperture telescopes. In principle, both the measurement noise and tilt jitter scale as $\sim t^{-1/2}$, translating each of these curves down with increasing exposure time. This suggests that, for a given pair of stars, if the differential offsets are dominated by tilt jitter for one integration time, they will be limited by it for all integration times.

The values in Figure 3 assume that tilt jitter is resolved by sufficiently short exposures. Longer exposure times will certainly reduce the differential tilt jitter by $1/\sqrt{t}$, but the measurement noise will also be decreased by this factor (for a given stellar brightness). The implication being that, if tilt jitter dominates for short exposure times, it will continue to dominate longer exposures.

The scaling laws demonstrated in Cameron, Britton, and Kulkarni (2008) indicate a substantially improved astrometric performance on large aperture telescopes equipped with adaptive optics. The expectations of astrometric precision for a field like M5 can be summarized by the expression

$$\sigma_{\text{tot}}^2 = \sigma_{\text{meas}}^2 + \sigma_{\text{TJ}}^2 = \left(\frac{1.4 \text{ sec}}{t} \right) \left\{ \left[1.7 \text{ mas} \left(\frac{2}{N} \right)^{0.3} \left(\frac{5 \text{ m}}{D} \right)^2 \right]^2 + \left[1.7 \text{ mas} \left(\frac{2}{N} \right)^{0.7} \left(\frac{5 \text{ m}}{D} \right)^{7/6} \right]^2 \right\}. \quad (10)$$

This equation assumes that measurement error is dominated by photon noise ($\propto D^{-2}$) and the other dependencies (stellar brightness distribution, turbulence profile) are identical to those for the Palomar M5 experiment.

Figure 4 shows the resulting estimates for astrometric precision as a function of aperture diameter and number of reference stars for 20sec of exposure time using Equation 10. The predictions are scaled using the results from Palomar, and agree well with those achieved at Keck. They also suggest that limits to astrometric precision arising from random errors lie below $10 \mu\text{as}$ for 30 m telescopes. However, very careful characterization and control of systematic errors will be required to achieve this level of precision in an actual experiment. The extent to which systematic errors can be eliminated will distinguish the scientific goals that can be accomplished with ground-based facilities from those that require a space-based solution.

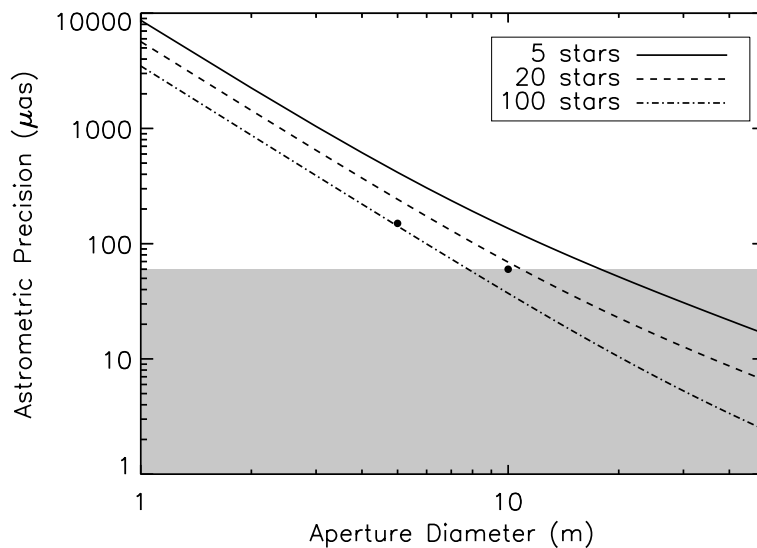


Figure 4. *Right Panel:* Astrometric precision as a function of aperture size and stellar density in 20 seconds of integration time. The points denote the levels of astrometric precision demonstrated at the Keck II and Palomar 200-inch telescopes. We have used Equation 10 with the assumptions of the Palomar turbulence profile, the M5 brightness distribution, and photon noise limit as described in §6. The astrometric precision demonstrates a very favorable scaling law with aperture diameter, and suggests orders of magnitude improvement in precision may be available using large aperture, AO equipped telescopes. In practice, the level of astrometric accuracy will depend on the extent to which current and future facilities can characterize and control systematic errors. The gray area denotes astrometric performance levels that have yet to be demonstrated with adaptive optics.

ACKNOWLEDGMENTS

We thank Nicholas Law, Michael Ireland, David Le Mignant, Adam Kraus, Marten van Kerkwijk, Andrew Gould, Andrea Ghez and Jessica Lu for useful discussions on astrometry. This work has been supported by NASA, and by the National Science Foundation Science and Technology Center for Adaptive Optics, managed by the University of California at Santa Cruz under cooperative agreement No. AST - 9876783.

REFERENCES

- [1] Cameron, P. B., Britton, M. C., and Kulkarni, S. R., “Precision Astrometry with Adaptive Optics,” *arXiv:0805.2153*; submitted to *The Astronomical Journal* **805** (May 2008).
- [2] Unwin, S. C., Shao, M., Tanner, A. M., Allen, R. J., Beichman, C. A., Boboltz, D., Catanzarite, J. H., Chaboyer, B. C., Ciardi, D. R., Edberg, S. J., Fey, A. L., Fischer, D. A., Gelino, C. R., Gould, A. P., Grillmair, C., Henry, T. J., Johnston, K. V., Johnston, K. J., Jones, D. L., Kulkarni, S. R., Law, N. M., Majewski, S. R., Makarov, V. V., Marcy, G. W., Meier, D. L., Olling, R. P., Pan, X., Patterson, R. J., Pitesky, J. E., Quirrenbach, A., Shaklan, S. B., Shaya, E. J., Strigari, L. E., Tomsick, J. A., Wehrle, A. E., and Worthey, G., “Taking the Measure of the Universe: Precision Astrometry with SIM PlanetQuest,” *Publications of the Astronomical Society of the Pacific* **120**, 38–88 (Jan. 2008).
- [3] Anderson, J. and King, I. R., “An Improved Distortion Solution for the Hubble Space Telescope’s WFPC2,” *Publications of the Astronomical Society of the Pacific* **115**, 113–131 (Jan. 2003).
- [4] Monet, D. G., Dahn, C. C., Vrba, F. J., Harris, H. C., Pier, J. R., Luginbuhl, C. B., and Ables, H. D., “U.S. Naval Observatory CCD parallaxes of faint stars. I - Program description and first results,” *The Astronomical Journal* **103**, 638–665 (Feb. 1992).
- [5] Pravdo, S. H. and Shaklan, S. B., “Astrometric Detection of Extrasolar Planets: Results of a Feasibility Study with the Palomar 5 Meter Telescope,” *The Astrophysical Journal* **465**, 264–+ (July 1996).

- [6] Anderson, J., Bedin, L. R., Piotto, G., Yadav, R. S., and Bellini, A., "Ground-based CCD astrometry with wide field imagers. I. Observations just a few years apart allow decontamination of field objects from members in two globular clusters," *Astronomy and Astrophysics* **454**, 1029–1045 (Aug. 2006).
- [7] Lazorenko, P. F., "Astrometric precision of observations at VLT/FORS2," *Astronomy and Astrophysics* **449**, 1271–1279 (Apr. 2006).
- [8] Gubler, J. and Tytler, D., "Differential Atmospheric Refraction and Limitations on the Relative Astrometric Accuracy of Large Telescopes," *Publications of the Astronomical Society of the Pacific* **110**, 738–746 (June 1998).
- [9] Lindegren, L., "Photoelectric astrometry - A comparison of methods for precise image location," in [*IAU Colloq. 48: Modern Astrometry*], Prochazka, F. V. and Tucker, R. H., eds., 197–217 (1978).
- [10] Diolaiti, E., Bendinelli, O., Bonaccini, D., Close, L. M., Currie, D. G., and Parmeggiani, G., "StarFinder: an IDL GUI-based code to analyze crowded fields with isoplanatic correcting PSF fitting," in [*Proc. SPIE Vol. 4007, p. 879-888, Adaptive Optical Systems Technology, Peter L. Wizinowich; Ed.*], Wizinowich, P. L., ed., *Presented at the Society of Photo-Optical Instrumentation Engineers (SPIE) Conference* **4007**, 879–888 (July 2000).
- [11] Britton, M. C., "The Anisoplanatic Point-Spread Function in Adaptive Optics," *Publications of the Astronomical Society of the Pacific* **118**, 885–900 (June 2006).
- [12] Betts, J. T., [*ACM Transactions on Mathematical Software*], ACM New York, NY —c1980, Vol 6, Issue 3 (1980).
- [13] Sasiela, R. J., [*Electromagnetic wave propagation in turbulence. Evaluation and application of Mellin transforms*], Springer Series on Wave Phenomena, Berlin: Springer, —c1994 (1994).
- [14] Hayward, T. L., Brandl, B., Pirger, B., Blacken, C., Gull, G. E., Schoenwald, J., and Houck, J. R., "PHARO: A Near-Infrared Camera for the Palomar Adaptive Optics System," *Publications of the Astronomical Society of the Pacific* **113**, 105–118 (Jan. 2001).
- [15] Troy, M., Dekany, R. G., Brack, G., Oppenheimer, B. R., Bloemhof, E. E., Trinh, T., Dekens, F. G., Shi, F., Hayward, T. L., and Brandl, B., "Palomar adaptive optics project: status and performance," in [*Proc. SPIE Vol. 4007, p. 31-40, Adaptive Optical Systems Technology, Peter L. Wizinowich; Ed.*], Wizinowich, P. L., ed., *Presented at the Society of Photo-Optical Instrumentation Engineers (SPIE) Conference* **4007**, 31–40 (July 2000).
- [16] Wizinowich, P., Acton, D. S., Shelton, C., Stomski, P., Gathright, J., Ho, K., Lupton, W., Tsubota, K., Lai, O., Max, C., Brase, J., An, J., Avicola, K., Olivier, S., Gavel, D., Macintosh, B., Ghez, A., and Larkin, J., "First Light Adaptive Optics Images from the Keck II Telescope: A New Era of High Angular Resolution Imagery," *Publications of the Astronomical Society of the Pacific* **112**, 315–319 (Mar. 2000).
- [17] Thomsen, M., Britton, M., and Pickles, A., "Mass-Dimm Setup at Palomar," in [*American Astronomical Society Meeting Abstracts*], *American Astronomical Society Meeting Abstracts* **210**, 117.01–+ (May 2007).
- [18] Kornilov, V., Tokovinin, A., Shatsky, N., Voziakova, O., Potanin, S., and Safonov, B., "Combined MASS-DIMM instruments for atmospheric turbulence studies," *Monthly Notices of the Royal Astronomical Society* **382**, 1268–1278 (Dec. 2007).
- [19] Cameron, P. B. and Kulkarni, S. R., "Kinematics of Magnetars," *in preparation* (2008).